

Mössbauer Study of the Three-Coordinate Planar Fe^{II} Thiolate Complex [Fe(SR)₃][−] (R = C₆H₂-2,4,6-tBu₃): Model for the Trigonal Iron Sites of the MoFe₇S₉:Homocitrate Cofactor of Nitrogenase

Yiannis Sanakis,^{†,‡} Philip P. Power,[§] Audria Stubna,[†] and Eckard Münck^{*,†}

Department of Chemistry, Carnegie Mellon University, 4400 Fifth Avenue, Pittsburgh, Pennsylvania 15213, Institute of Materials Science, NCSR “Demokritos”, 15310 Ag. Paraskevi, Attiki, Greece, Department of Biological Applications and Technologies, University of Ioannina, 45110 Ioannina, Greece, and Department of Chemistry, University of California, Davis, California 95616

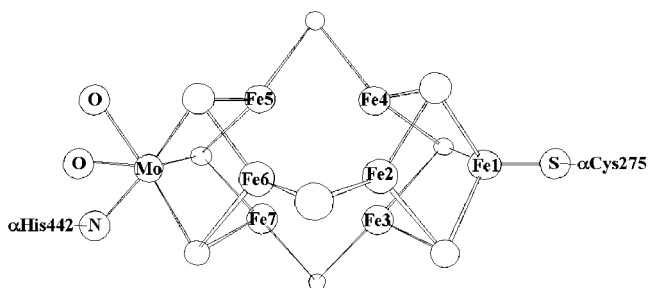
Received October 31, 2001

The cofactor (M-center) of the MoFe protein of nitrogenase, a MoFe₇S₉:homocitrate cluster, contains six Fe sites with a (distorted) trigonal sulfido coordination. These sites exhibit unusually small quadrupole splittings, $\Delta E_Q \approx 0.7$ mm/s, and isomer shifts, $\delta \approx 0.41$ mm/s. Mössbauer and ENDOR studies have provided the magnetic hyperfine tensors of all iron sites in the $S = 3/2$ state M^N . To assess the intrinsic zero-field splittings and hyperfine parameters of the cofactor sites, we have studied with Mössbauer spectroscopy two salts of the three-coordinated Fe^{II} thiolate complex [Fe(SR)₃][−] (R = C₆H₂-2,4,6-tBu₃). One of the salts, [Ph₄P][Fe(SR)₃][−]·2MeCN·C₇H₈, **1**, has a planar geometry with idealized C_{3h} symmetry. This $S = 2$ complex has an axial zero-field splitting with $D = +10.2$ cm^{−1}. The magnetic hyperfine tensor components $A_x = A_y = -7.5$ MHz and $A_z = -29.5$ MHz reflect an orbital ground state with d_z^2 symmetry. $A_{iso} = (A_x + A_y + A_z)/3 = -14.9$ MHz, which includes the contact interaction ($\kappa P = -21.9$ MHz) and an orbital contribution (+7 MHz), which is substantially smaller than $A_{iso} \approx -22$ MHz of the tetrahedral Fe^{II}(S–R)₄ sites of both rubredoxin and [PPh₄]₂[Fe^{II}(SPh)₄]. The largest component of the electric field gradient (EFG) tensor is negative, as expected for a d_z^2 orbital. However, $\Delta E_Q = -0.83$ mm/s, which is smaller than expected for a high-spin ferrous site. This reduction can be attributed to a ligand contribution, which in planar complexes provides a large positive EFG component perpendicular to the ligand plane. The isomer shift of **1**, $\delta = 0.56$ mm/s, approaches the δ -values reported for the six trigonal cofactor sites. The parameters of **1** and their importance for the cofactor cluster of nitrogenase are discussed.

Introduction

Iron sulfur clusters are found in all living organisms. The vast majority of clusters contain Fe^{II}/Fe^{III} sites with tetrahedral cysteinyl/sulfido coordination.¹ The sole exception is the cofactor (M-center) of the MoFe protein of nitrogenase, Chart 1, a MoFe₇S₉:homocitrate cluster containing six Fe sites with distorted, trigonal sulfido coordination and one Fe site, bound to Cys275, with tetrahedral FeS₃(Cys)

Chart 1



coordination.² The cofactor cluster of nitrogenase has been studied with a variety of spectroscopic techniques, including Mössbauer spectroscopy.³ Because the clusters from the

* To whom correspondence should be addressed. E-mail: em40@andrew.cmu.edu. Fax: (412) 268-1061.

[†] Carnegie Mellon University.

[‡] Institute of Materials Science, NCSR “Demokritos”, and University of Ioannina.

[§] University of California.

(1) (a) Beinert, H.; Holm, R. H.; Münck, E. *Science* **1997**, *277*, 653. (b) Cammack, R. *Adv. Inorg. Chem.* **1992**, *38*, 281.

(2) Howard, J. B.; Rees, D. C. *Chem. Rev.* **1996**, *96*, 2965.

various organisms have nearly the same Mössbauer parameters, we quote here the parameters obtained for the MoFe protein from *Azotobacter vinelandii*, the protein most extensively studied.⁴ The trigonal sites of the *A. vinelandii* cluster have $\Delta E_Q = 0.70$ mm/s (independent of temperature) and $\delta = 0.41$ mm/s (at 4.2 K relative to Fe metal at room temperature). Recent analyses of Q-band ENDOR data⁵ and Mössbauer data,⁴ obtained for MoFe protein where only the M-center (but not the Fe₈S₇ P-cluster) was enriched with the Mössbauer isotope ⁵⁷Fe, suggest that the majority,⁴ if not all,⁵ of the trigonal sites are high-spin ferrous. Given that a three-coordinate site should yield a high-spin ($S = 2$) configuration, the small quadrupole splittings have been puzzling. Moreover, for high-spin ferrous sites, the isomer shifts are also remarkably small.⁶ Finally, while the effective magnetic hyperfine tensors, **A**, of all iron sites have been determined by Mössbauer and ENDOR spectroscopy, we do not know the intrinsic **A**-values for a ferrous or ferric site with trigonal sulfido coordination. The lack of intrinsic **A**-values for such sites is a strong impediment for testing spin-coupling models for the $S = 3/2$ state of the M-center.

In 1995, Power, Holm, and co-workers⁷ published the synthesis and structure of the trigonal planar Fe^{II} thiolate complex, [Fe(SR)₃]⁻ (R = C₆H₂-2,4,6-tBu₃), which has been crystallized as two salts. The Fe site of [Ph₄P][Fe(SR)₃]·2MeCN·C₇H₈, **1**, exhibits a slightly distorted planar geometry with idealized C_{3h} symmetry; the S–Fe–S bond angles range from 116.6° to 121.9°, and the Fe–S distances average 2.274(7) Å. Complex **1** exhibits $\Delta E_Q = 0.81$ mm/s and $\delta = 0.57$ mm/s⁷ and thus has parameters reminiscent of the trigonal cofactor sites. Its room-temperature moment is 5.05 Bohr magnetons, indicative of a $S = 2$ site. The second salt, [Li(THF)₂Fe(SR)₃]·1/2C₆H₁₄, **2**, also has a near planar trigonal environment at the iron. The axial symmetry, however, is significantly distorted by a lithium ion bridging two of the thiolato sulfurs; the resulting S–Fe–S angles are 92.2°, 123.2°, and 141.7°.⁷ Moreover, the two Fe–S distances that involve the bridged sulfurs average 2.325(10) Å and are significantly longer than the nonbridging Fe–S bond of 2.259(4) Å.

In this manuscript, we report a comprehensive Mössbauer investigation of high-spin ferrous **1** and **2**, from which we have extracted zero-field splittings (ZFS), **A**-tensors, isomer shifts, and electric field gradient (EFG) tensors. The isotropic portion of the **A**-tensors, A_{iso} , of **1** and **2** were found to be substantially smaller than those of $S = 2$ tetrahedral tetrathiolate complexes. The ground state of **1** is a d_{z^2} orbital

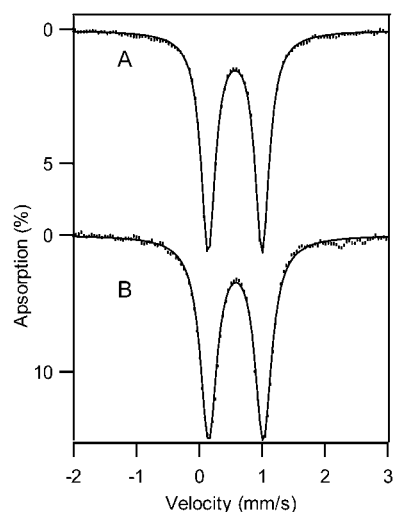


Figure 1. Mössbauer spectra of polycrystalline **1** (A, 4.2 K) and **2** (B, 80 K) recorded in zero field. The solid lines are spectral simulations using the parameters listed in Table 1. (Lorentzian line width of 0.27 mm/s (fwhm) for **1** and 0.32 mm/s for **2**).

that produces a negative and axial quadrupole splitting. The small EFG of **1** results from a strong ligand contribution from the planar ligand system, which opposes the valence contribution of the d_{z^2} ground state.

Materials and Methods

Complexes **1** and **2**, extremely air and moisture sensitive crystalline solids, were prepared as described previously⁷ and handled under anaerobic and anhydrous conditions. The authenticity of **1** and **2** were verified by checking the cell constants of crystalline samples. Good combustion analysis data were difficult to obtain owing to desolvation of the crystals upon pumping under vacuum.

The samples were fixed in the Mössbauer cuvettes by stirring the polycrystalline powders into degassed paraffin. Mössbauer spectra were recorded in two spectrometers that allowed variation of the temperature between 1.5 and 200 K in parallel applied magnetic fields up to 8.0 T. The spectra were analyzed using the software WMOSS (WEB Research Co., Edina, MN).

Results

Figure 1A shows a Mössbauer spectrum of a polycrystalline sample of **1** recorded at 4.2 K in the absence of an applied magnetic field. The spectrum consists of a doublet with quadrupole splitting $\Delta E_Q = 0.83(2)$ mm/s and isomer shift $\delta = 0.56(2)$ mm/s. ΔE_Q was found to be independent of temperature up to 150 K. Within the uncertainties, these values agree with $\Delta E_Q = 0.81$ mm/s and $\delta = 0.57$ mm/s reported by MacDonnell and co-workers.⁷ However, the sample contains an unknown contaminant, which appears as a quadrupole doublet with $\Delta E_Q \approx 1.2$ mm/s and $\delta \approx 0.4$ mm/s above 20 K (not shown). This contaminant accounts for ~9% of the Fe in the sample and is paramagnetic, contributing at 4.2 K to broad unresolved features that extend over a 12–15 mm/s velocity range. Because the absorption of this contaminant is spread out, it does not interfere with the analysis of the low-temperature spectra of **1**.

We have recorded 4.2 K spectra in parallel applied fields up to 8.0 T, a 1.5 K spectrum at 3.0 T, and 8.0 T spectra at

(3) Burgess, B. K. *Chem. Rev.* **1990**, *90*, 1377.

(4) Yoo, S. J.; Angove, H. C.; Papaefthymiou, V.; Burgess, B. K.; Münck, E. *J. Am. Chem. Soc.* **2000**, *122*, 4926.

(5) Lee, H.-I.; Hales, B. J.; Hoffman, B. M. *J. Am. Chem. Soc.* **1997**, *119*, 11395.

(6) Isomer shifts of octahedral Fe^{II} sites with N/O coordination have $\delta \approx +1.15$ – 1.30 mm/s, whereas high-spin ferrous Fe^{II}(SR)₄ sites exhibit δ values around 0.70 mm/s. Isomer shifts decrease with decreasing coordination number; thus, the low δ values of the trigonal cofactor sites did not appear that unusual after the X-ray structure became available. However, there is still a paucity of Mössbauer parameters of three-coordinate Fe complexes.

(7) MacDonnell, F. M.; Ruhlandt-Senge, K.; Ellison, J. J.; Holm, R. H.; Power, P. P. *Inorg. Chem.* **1995**, *34*, 1815.

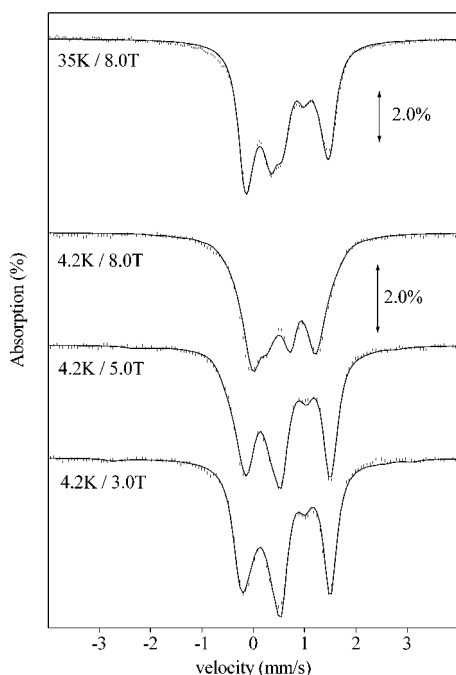


Figure 2. Mössbauer spectra of **1** recorded in parallel applied magnetic fields and at temperatures indicated. The solid lines are spectral simulations based on eq 1 using the parameters listed in Table 1.

35, 50, 100, and 150 K; representative spectra are shown in Figure 2. The spectra shown in Figure 2 exhibit paramagnetic hyperfine structure that depends both on the applied field and the temperature. We have analyzed the spectra in the framework of the $S = 2$ spin Hamiltonian.

$$H = [D(S_z^2 - 2) + E(S_x^2 - S_y^2)] + \beta \mathbf{S} \cdot \mathbf{g} \cdot \mathbf{B} + \mathbf{S} \cdot \mathbf{A} \cdot \mathbf{I} + H_Q - g_n \beta_n \mathbf{B} \cdot \mathbf{I} \quad (1)$$

with

$$H_Q = \frac{eQV_{zz}}{2} [3I_z^2 - 15/4 + \eta(I_x^2 - I_y^2)] \quad (2)$$

In eqs 1 and 2, all symbols have their conventional meanings.

Our analysis suggests that the electronic spin relaxes slowly at 4.2 K and fast for $T > 30$ K. The major spectral features are determined by the internal magnetic field $\mathbf{B}_{\text{int}} = -\langle \mathbf{S} \rangle \cdot \mathbf{A} / g_n \beta_n$ where $\langle \mathbf{S} \rangle$ is the expectation value of the electronic spin. The field dependence of the Mössbauer spectra readily establishes that the zero-field splitting parameter D is positive and roughly 10 cm^{-1} . We also expect from the near trigonal symmetry that the rhombic ZFS parameter E is approximately zero. Thus, the $M_S = 0$ spin level is the ground state. This level produces in zero field $\langle S \rangle = \langle 2,0 | S | 2,0 \rangle = 0$, where we used the standard $|S, M_S\rangle$ nomenclature. For $D \approx 10 \text{ cm}^{-1}$, the applied field mixes the $M_S = \pm 1$ levels into the ground state, yielding finite expectation values for $\langle S_x \rangle$ and $\langle S_y \rangle$ (ca. -1.8 at 8.0 T) while $\langle S_z \rangle$ remains near zero. Hence, the low-temperature data are sensitive to D , A_x , and A_y . At higher temperatures, $\langle \mathbf{S} \rangle$ has to be thermally averaged over all accessible spin levels, denoted $\langle \mathbf{S} \rangle_{\text{th}}$. For $kT \gg D$, the thermally averaged spin obeys the Curie law.⁸ Under these conditions, $\langle \mathbf{S} \rangle_{\text{th}}$ is essentially

Table 1. Mössbauer Parameters for Complexes **1** and **2**^a

	1	2
D (cm^{-1})	10.2(5)	14(3)
E/D	0	0.25
δ (mm/s)	0.56(1)	0.60(1)
ΔE_Q (mm/s)	-0.83(2)	-0.87(2)
η	0	0.93(7)
α_{EFG} (deg)	0	40
A_x (MHz)	-7.5(4)	-3.9 ^b
A_y (MHz)	-7.5(4)	+4.5 ^b
A_z (MHz)	-29.5(14)	-36(4)
A_{iso} (MHz)	-14.9	-11.8
α_A (deg)	0	60

^a The numbers in parentheses give estimated uncertainties of the last significant digits. ^b A_x and A_y of **2** depend on the choice of D and on the rotation of the EFG and \mathbf{A} -tensor around the electronic z -axis (angles α_{EFG} and α_A). However, the magnitude of both A_x and A_y are smaller than 5 MHz.

independent of D and E , and by measuring \mathbf{B}_{int} at higher temperatures, the principal components of the \mathbf{A} -tensor can be estimated. At 4.2 K, \mathbf{B}_{int} depends linearly on \mathbf{A} and inversely on D , except at high fields, where $\langle \mathbf{S} \rangle$ approaches saturation. Thus, by estimating the \mathbf{A} -tensor components at higher temperatures, the magnitude of D can be determined at 4.2 K with good precision ($\pm 10\%$). Finally, at 35 K, the z -component, $\langle S_z \rangle_{\text{th}}$, has a sizable contribution from the $M_S = -1$ level, providing for an accurate determination of A_z .

The solid lines in Figure 2 are computer simulations based on eq 1. After obtaining approximate values for all parameters, we have simultaneously least-squares fit groups of four spectra. The parameters obtained are listed in Table 1. We have explored both the axial and rhombic cases but found that abandoning axial symmetry only marginally improved the fits. The essential results are as follows: The largest component of the electric field gradient (EFG) tensor is negative, suggesting an orbital ground state of d_{z^2} symmetry. A_x and A_y are rather small compared to A_z , leading to the relatively small splittings observed in the data of Figure 2.

Mössbauer spectra of the lithium salt, **2**, are shown in Figures 1B and 3. Similar to **1**, the polycrystalline sample of **2** also contains a minor contaminant that can be recognized in the 4.2 K spectra, where it produces a shallow absorption extending from -5 mm/s to $+5 \text{ mm/s}$ Doppler velocity. The presence of the contaminant is also indicated by some absorption at -0.3 mm/s and $+2.2 \text{ mm/s}$ in the 80 K spectrum of Figure 1B. In general, the fits for the spectra of **2** are of lower quality than those of complex **1**. In particular, even after abandoning rhombic symmetry, we have not been able to model the peak at $\approx +1.1 \text{ mm/s}$ Doppler velocity in the 3.0, 6.0, and 8.0 T low temperature spectra. Moreover, the high-energy shoulder in these spectra is not simulated well. (The sloping high-energy features are likely caused by a distribution of D . Because the orbital contribution to the magnetic hyperfine tensor is correlated to D , see later, A_x and A_y would also be distributed, contributing to the

(8) Kauffmann, K. E.; Münck, E. In *Spectroscopic Methods in Bioinorganic Chemistry*; Solomon, E. I., Hodgson, K., Eds.; ACS Symposium Series 692; American Chemical Society: Washington, DC, 1998; p 16.

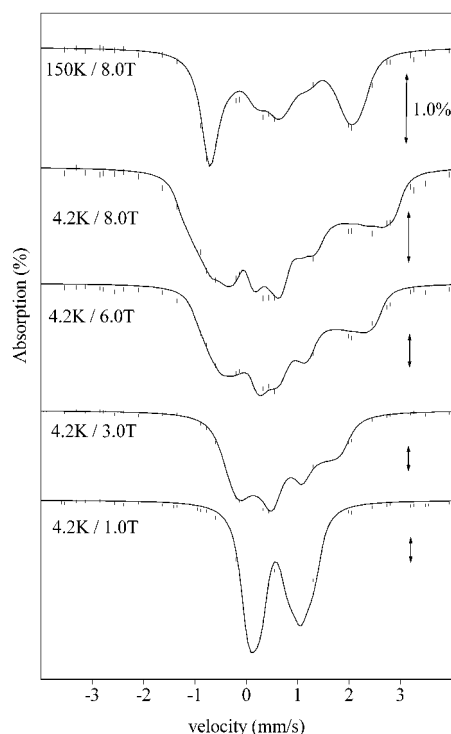


Figure 3. Mössbauer spectra of **2** in parallel applied magnetic fields and temperatures indicated. The solid lines are spectral simulations based on eq 1 using the parameters listed in Table 1.

spreading of the absorption features.) Because the symmetry of **2** is low, we have allowed the **A**-tensor and EFG tensor to be rotated relative to the ZFS tensor. However, **2** has idealized C_S symmetry, and thus, all tensors must have one principal axis normal to the reflection plane. Therefore, for the final fits, the rotations were confined to α_{EFG} and α_{A} around the z -axis. Although the simulations shown in Figure 3 are far from perfect, the essential features are all represented. The values of some parameters were quite robust under the various fitting procedures. For instance, D was generally found to be in the range of 11 to 16 cm^{-1} . From the 8.0 T spectrum recorded at 150 K, $A_z = -36 \pm 4$ MHz was determined. The magnitudes of both A_x and A_y were found to be below 5 MHz, and A_y was always positive. Because A_x and A_y are small, the spectra are not very sensitive to the value of E/D (which controls the spin expectation values in the xy plane); the E/D value can readily be changed provided it is compensated for by readjustment of A_x and A_y .

Discussion

The goal of the present work was to study the zero-field splittings and the hyperfine interactions of a complex with trigonal sulfur coordination. The study of these interactions is of particular interest because of the (near) trigonal coordination observed for six Fe sites of the nitrogenase M-center. Without knowledge about the intrinsic **A**-values, it is extremely difficult to construct spin coupling schemes that elucidate the electronic structure of the M-center in the $S = 3/2$ state M^N , the state intensively studied with a variety of spectroscopic techniques. Moreover, as pointed out in a

previous section, most, if not all, of the trigonal sites are suspected to be high-spin ferrous, and thus, it has been surprising that the observed quadrupole splittings for these sites are ~ 0.7 mm/s rather than 2.5–3.5 mm/s as expected for typical high-spin ferrous, tetrahedral sites. Finally, for a more detailed analysis of the spin coupling, one has to know the magnitude of the zero-field splittings. Because the ZFS tensors of the individual iron sites do not commute with the exchange interactions, the zero-field splitting terms can mix spin multiplets leading to substantially altered magnetic hyperfine interactions.⁹ If such mixing remains unrecognized, substantial errors are introduced into the spin coupling analysis. In the following, we address these questions.

As pointed out in the Results section, ΔE_Q of **1** is independent of temperature between 4.2 and 150 K, indicating that the electronic ground state is an isolated orbital singlet.¹⁰ In C_{3h} symmetry, the d-orbitals split into a singlet (A'_1, d_{z^2}) and two orbital doublets (E', E''). Thus, the orbital ground state of **1** has d_{z^2} symmetry, where z is perpendicular to the plane of the three sulfur atoms coordinated to the iron. Because the system has an isolated orbital ground state and the $S = 2$ spin multiplet does not exhibit excessively large zero-field splittings ($D \approx 10$ cm^{-1}), the ZFS, g -, and **A**-tensors can be analyzed with a spin Hamiltonian derived by treating spin–orbit coupling ($\lambda \mathbf{L} \cdot \mathbf{S}$), the electronic Zeeman interactions, and the magnetic hyperfine term in perturbation up to second order (see eq 19.32 of ref 12). For the present axial case, this treatment yields the following expressions:

$$D = 3\lambda^2/\Delta \quad (3)$$

where $\lambda = -103$ cm^{-1} is the spin–orbit coupling constant of the free Fe^{II} ion and Δ is the energy difference between the d_{z^2} ground state and the degenerate pair of (d_{xz}, d_{xy}) levels. For the g -tensor, we obtain the expressions

$$g_z = 2.00 \text{ and } g_{\perp} = g_z - 3\lambda/\Delta \quad (4)$$

and using eq 3

$$g_{\perp} = 2(1 - D/\lambda) \quad (5)$$

The components of the **A**-tensor are given by

$$A_z = -\kappa P - (1 - B^2)P/7 \approx -\kappa P - P/7 \quad (6)$$

- (9) (a) Sage, J. T.; Xia, Y.-M.; Debrunner, P. G.; Keough, D. T.; DeJersey J.; Zerner, B. *J. Am. Chem. Soc.* **1989**, *111*, 7239. (b) Fox, B. G.; Hendrich, M. P.; Surerus, K. K.; Andersson, K. K.; Froland, W. A.; Lipscomb, J. D.; Münck, E. *J. Am. Chem. Soc.* **1993**, *115*, 3688. (c) Bencini A.; Gatteschi D. *EPR of Exchanged Coupled Systems*; Springer-Verlag: New York, 1990.
- (10) This argument is a bit simplistic but correct when the ZFS parameters are also taken into account. We have shown recently¹¹ that an isolated singlet results for an orbitally degenerate case by action of spin–orbit coupling. This orbitally degenerate case yields an extremely large ($-D > 50$ cm^{-1}) and negative zero-field splitting rather than the positive D observed here.
- (11) Andres, H.; Bominaar, E. L.; Smith, J. M.; Eckert, N. A.; Holland, P. L.; Münck, E. *J. Am. Chem. Soc.* **2002**, *124*, 3012.
- (12) Abragam, A.; Bleaney, B. *Electron Paramagnetic Resonance of Transition Ions*; Dover Publications: New York, 1986.

$$A_{\perp} = -\kappa P + (g_{\perp} - 2)P + (1 - B^2)P/14 \approx -\kappa P + (g_{\perp} - 2)P + P/14 \quad (7)$$

where $P = N\beta\beta_n\langle r^{-3} \rangle$ is a scaling factor that depends on the radial extension of the d-orbitals and N is a covalency factor. In eqs 6 and 7, the first term ($-\kappa P$) describes the Fermi contact contribution, $(g_{\perp} - 2)P$ gives the orbital contribution to the **A**-tensor, and $-P/7$ and $P/14$ result from the traceless spin-dipolar interaction. The spin-dipolar term has a second-order contribution, B^2 , that can be estimated from the measured ZFS to be $B^2 \approx 0.02$ and can thus be neglected for the present discussion.

Both the axial nature and the large magnitude of D for **1** prevent the determination of the g -values by X- and Q-band EPR. (It would be worthwhile to measure the g -values at frequencies above 200 GHz.) As long as mixing of the $^5A'$ ground state with $S = 1$ configurations can be ignored, g_{\perp} can be obtained from D and λ by means of eq 5, yielding $g_{\perp} = 2.20$ for complex **1**.¹³ With this information, we can calculate P and κ from eqs 6 and 7. Our experimental result (Table 1) of $A_{\perp} = -7.5$ MHz and $A_z = -29.5$ MHz yields $P = 53.1$ MHz and $\kappa = 0.41$. Interestingly, the value of κ agrees very well with the $\kappa = 0.43$ calculated for the free Fe^{II} ion.¹⁷

In analyses commonly used to assess a spin coupling scheme, one works with the isotropic part of the magnetic hyperfine interaction, $A_{\text{iso}} = (A_x + A_y + A_z)/3$; taking the trace of **A** removes the contribution of the traceless dipolar term, yielding $A_{\text{iso}} = -14.9$ MHz for **1**. A_{iso} contains a contribution from the isotropic Fermi contact term as well as an isotropic (pseudocontact) contribution from the orbital term that opposes the Fermi contact term.¹² $A_{\text{contact}} (-\kappa P = -21.9$ MHz for **1**) depends primarily on the covalency and thus might be expected to remain rather constant for sites with similar ligand structure. On the other hand, the orbital contribution to A_{iso} , $A_L = P(\text{tr}(\mathbf{g} - 2))/3 = 0.133P = +7$ MHz for **1**, will depend on the orbital energies and thus is expected to be more sensitive to structural differences. A_{iso} is the quantity that is generally used in spin-coupling models to analyze, in conjunction with spin projection factors (see for instance ref 18), the magnetic hyperfine interactions of

exchange-coupled clusters. Thus, considering the lack of other model systems, $A_{\text{iso}} \approx -15$ MHz (or even a slightly smaller value, see later) might be an appropriate value representing the intrinsic **A**-values of the trigonal Fe^{II} sites of the M-center. It is noteworthy that while A_{iso} of **1** is comparable to $A_{\text{iso}} \approx -16.6$ MHz deduced for the Fe^{II} sites of $[\text{2Fe}-\text{2S}]^{1+}$ clusters (see Table 5 of ref 18), it is substantially smaller than $A_{\text{iso}} = -21.6$ MHz of tetrahedral Fe^{II} sites of rubredoxin and its model complexes.^{18,19} The complex $[\text{PPh}_4]_2[\text{Fe}^{\text{II}}(\text{SPh})_4]$ has proven to be an excellent model for the electronic structure of the Fe^{II} site of reduced rubredoxin. Recently, the g -values of this complex were determined by high-frequency EPR.²⁰ Using these g -values and recent rubredoxin Mössbauer data obtained in our laboratory, we obtain $P = 63$ MHz. The small value of P obtained for **1** indicates a more covalent site than observed in $\text{Fe}^{\text{II}}(\text{thiolato})_4$ complexes. Although this suggestion has still to be explored with appropriate quantum chemical calculations (which unfortunately do not yield good values for A_{contact}), it should be noted that **1** does have substantially shorter Fe–S bonds (average 2.27 Å) than the Fe^{II} site of rubredoxin (average 2.36 Å).²⁵ For comparison, the average Fe–S distance for the trigonal M-center sites is 2.24 Å as inferred from the 1.6 Å data of the *Klebsiella pneumoniae* protein.²⁶

The zero-field splitting parameter of **1**, $D = 10.2$ cm^{-1} , is quite large, and if this value would apply to the trigonal M-center sites, the spin expectation values of the latter could depend strongly on the zero-field splitting parameters in case the, as yet unknown, exchange coupling constants are comparable to D . The D -value of **1** can be used to estimate the orbital energies of the (d_{xz} , d_{xy}) doublet. Using eq 3 and the free ion value of λ , we find that these levels are roughly at energy 3000 cm^{-1} .

As can be seen by inspection of Table 1, ΔE_Q and δ are quite similar for both **1** and **2**. However, the EFG tensor of

- (13) Solomon and collaborators¹⁴ have shown for $\text{Fe}(\text{SR})_4$ ($R = 2\text{-PhC}_6\text{H}_4$), a ferrous complex with tetrahedral thiolate coordination, that low-lying $^3\Gamma$ states can mix into the 5E_g ground states, contributing -1.5 cm^{-1} to the zero-field splitting of the complex ($D = -8.7$ cm^{-1}). The frequently used correlation between the zero-field splitting parameters D and E and the g -tensor, $g_{yx} = g_z - 2k(D \pm E)/\lambda$,¹⁵ is quite useful to estimate the g -values if EPR data are not available. However, four corrections affect this relation: (i) the expressions for g and the zero-field splitting parameters might contain contributions from low-lying triplet states,¹⁴ (ii) the ZFS parameters, but not g , have a contribution (ρ) from intra-atomic spin–spin interactions,¹² (iii) the orbital reduction factor k is generally not known, and (iv) λ is covalently reduced from the free ion value. We have found deviations from this equation for the C42S rubredoxin mutant for which we have determined by EPR that $g_z = 2.08(1)$.¹⁶
- (14) Gebhard, M. S.; Koch, S. A.; Millar, M.; Devlin, F. J.; Stephens, P. J.; Solomon, E. I. *J. Am. Chem. Soc.* **1991**, *113*, 1640.
- (15) Zimmermann, R.; Spiering, H.; Ritter, G. *Chem. Phys.* **1974**, *4*, 133.
- (16) Yoo, S. J.; Meyer, J.; Achim, A.; Peterson, J.; Hendrich, M. P.; Münck, E. *J. Biol. Inorg. Chem.* **2000**, *5*, 475.
- (17) Freeman, A. J.; Watson, R. E. In *Magnetism*; Rado, G. T.; Suhl, H., Eds.; Academic Press: New York, 1965; Vol. IIA.

- (18) Mouesca, J. M.; Noodleman, L.; Case, D. A.; Lamotte, B. *Inorg. Chem.* **1995**, *34*, 4347.
- (19) A recent high-frequency EPR study²⁰ of the rubredoxin model complex $[\text{PPh}_4]_2[\text{Fe}^{\text{II}}(\text{SPh})_4]^{2+}$ yielded $D = 5.84$ cm^{-1} , $E/D = 0.24$, $g_x = g_y = 2.08$, and $g_z = 2.00$. This model complex has essentially the same hyperfine parameters as reduced rubredoxin;²² however, the D -value of the model is substantially smaller than the value $D = 7.8$ cm^{-1} reported for rubredoxin from *C. pasteurianum*.²³ We have recently reinvestigated this protein with Mössbauer spectroscopy using applied fields up to 8.0 T.²⁴ Our data analysis yields $D = 5.7(3)$ cm^{-1} , a value in excellent agreement with that obtained for the model compound. Moreover, our study yields a slightly improved value for A_{iso} , namely $A_{\text{iso}} = -21.6$ MHz. Our analysis indicates also that nearly 40% of the D -value of rubredoxin is contributed by mixing with excited triplet states.
- (20) Knapp, M. J.; Krzystek, J.; Brunel, L.-C.; Hendrickson, D. N. *Inorg. Chem.* **2000**, *39*, 281.
- (21) Coucouvanis, D.; Swenson, D.; Baenziger, N. C.; Murphy, C.; Holah, D. G.; Sfarnas, N.; Simopoulos, A.; Kostikas, A. *J. Am. Chem. Soc.* **1981**, *103*, 3350.
- (22) Winkler, H.; Bill, E.; Trautwein, A. X.; Kostikas, A.; Simopoulos, A.; Terzis, A. *J. Chem. Phys.* **1988**, *89*, 732.
- (23) Schulz, C.; Debrunner, P. G. *J. Phys.* **1976**, *C6-37*, 253. (b) Winkler, H.; Schulz, C.; Debrunner, P. G. *Phys. Lett.* **1979**, *69A*, 360.
- (24) Vrajmasu, V.; Bominaar, E. L.; Meyer, J.; Münck, E. In preparation.
- (25) Min, T.; Ergenekan, C. E.; Eidsness, M. K.; Ichiye, T.; Kang, C. *Protein Sci.* **2001**, *10*, 613.
- (26) Mayer, S. M.; Lawson, D. M.; Gormal, C. A.; Roe, S. M.; Smith, B. E. *J. Mol. Biol.* **1999**, *292*, 871.

2 shows that the complex has rhombic, or probably lower, symmetry. Interestingly, $A_{\text{iso}} = -11.8$ MHz of **2** is substantially smaller than $A_{\text{iso}} = -14.9$ MHz of **1**. The smaller A_{iso} value of **2** may reflect a larger pseudocontact contribution. From the relation $g_{y,x} = 2.00 - 2(D \pm E)/\lambda$, and using $P = 53$ MHz, we can estimate $A_{\text{L}} = +9.6$ MHz for **2**. Thus, compared to **1**, the A_{iso} value of **2** would be reduced by an additional 2.5 MHz, a reduction in good agreement with the data.²⁷

The magnetic hyperfine interaction of **1** fits very well to a d_{z^2} ground state. For this state, one expects an axial and negative quadrupole interaction with $\Delta E_{\text{Q}} \approx -(2.5 - 3.5)$ mm/s. For instance, the high-spin ferrous site of rubredoxin exhibits $\Delta E_{\text{Q}} = -3.23$ mm/s, and in fact, most high-spin ferrous complexes have $|\Delta E_{\text{Q}}|$ values above 2.5 mm/s. Thus, the small ΔE_{Q} values of the trigonal sites of the M-center, $\Delta E_{\text{Q}} \approx 0.7$ mm/s, and the small ΔE_{Q} values of **1** and **2** have been puzzling. However, it has recently become quite apparent to us that complexes with approximately planar ligand systems exhibit quadrupole splittings with large ligand contributions. Such contributions are best appreciated with reference to some planar ferric complexes. The ground state of the high-spin Fe^{III} ion has a ^6S parentage for which the valence contribution to the EFG is (ideally) zero. However, a variety of planar Fe^{III} complexes exhibit large ΔE_{Q} values, such as iron porphyrins ($\Delta E_{\text{Q}} = +1$ to $+2$ mm/s)²⁸ and $\text{Fe}[\text{N}(\text{SiMe}_3)_2]_3$ ($\Delta E_{\text{Q}} = +5.12$ mm/s).²⁹ A vanishing valence contribution to the EFG is also predicted for intermediate spin ($S = 3/2$) Fe^{III} complexes in which the unpaired $d_{x^2-y^2}$ electron of the $S = 5/2$ state is substituted by a spin-paired d_{xy} electron. Examples are found for several iron porphyrins²⁸ and for $[\text{FeCl}(\eta^4\text{-MAC}^*)]^{2+}$ ($\Delta E_{\text{Q}} = +3.6$ mm/s).³⁰ These examples show that planar ligands produce a large positive EFG component normal to the ligand plane. We have recently analyzed in some detail¹¹ the ligand contribution for a series of planar complexes $[\text{LFe}^{\text{II}}\text{X}]^0$ ($\text{L} = \beta$ -diketiminate; $\text{X} = \text{Cl}^-$, CH_3^- , NHTol^- , NHtBu^-) and found by crystal field analysis and density functional theory (DFT) calculations¹¹ that such ligand arrangements indeed give a substantial positive ligand EFG component normal to the ligand plane. The DFT calculations, well suited to the problem because the field gradient depends on the charge distribution, gave similar ligand contributions in the ferrous

state. If we apply these considerations to **1** in a qualitative way, we expect a substantial reduction of ΔE_{Q} due to the positive ligand contribution opposing the negative valence contribution. Extrapolating to the trigonal Fe sites of M^{N} , the present considerations give a rational, but not yet quantitative, explanation of the small ΔE_{Q} values reported for the M-center.³¹

The isomer shift measures the s-electron density at the nucleus, and because this quantity is strongly influenced by electrostatic shielding of valence d electrons, δ is generally a good indicator of both oxidation state and coordination number. The shifts of **1**, $\delta = 0.56(1)$ mm/s, and **2**, $\delta = 0.60(1)$ mm/s, are lower than those of high-spin ferrous complexes with tetrahedral sulfur coordination ($\delta = 0.70$ mm/s for the $\text{Fe}^{\text{II}}(\text{Cys})_4$ of rubredoxin and $\delta = 0.71$ mm/s for the $\text{Fe}^{\text{II}}(\text{Cys})_2(\text{S}^{2-})_2$ sites of the all-ferrous Fe_2S_2 cluster from *Aquifex aeolicus*).³³ To date, **1** is the only synthetic complex with trigonal thiolato coordination, and thus, its isomer shift has particular relevance to the electronic structure of the nitrogenase cofactor. We have previously argued,⁴ on the basis of comparing the nitrogenase sites with that of **1**, that the isomer shifts of the cofactor sites, $\delta_{\text{av}} = 0.41$ mm/s, suggest a $\text{Mo}^{\text{IV}}4\text{Fe}^{\text{II}}3\text{Fe}^{\text{III}}$ oxidation state for the $S = 3/2$ form of the cofactor cluster, rather than $\text{Mo}^{\text{IV}}6\text{Fe}^{\text{II}}\text{Fe}^{\text{III}}$ as proposed by Lee et al.⁵ Some questions arise in using the δ -value of **1** to assess the oxidation state of the M-center. For instance, the trigonal M-center sites have sulfido rather than thiolato coordination. Replacement of two thiolato groups with sulfido ligands seems to have little effect on δ for the tetrahedral sites, as witnessed by the observation that the Fe^{II} sites of rubredoxin and the all-ferrous $[\text{2Fe}-\text{2S}]$ cluster from *Aquifex aeolicus*³³ have the same δ -value. (In the mixed-valence states of the Fe-S clusters, the δ -values of the ferrous sites are reduced by partial delocalization toward the ferric sites; ref 34.) Also, one should keep in mind that ligands **1** and **2** are thiophenolates for which the electronic structure of the sulfur is influenced by conjugation with the aromatic ring.¹⁴ Further, the M-center is a polynuclear cluster with metal-metal interactions that are likely to exhibit increased covalency of the sites. Covalency and valence delocalization are important features of the electronic structure as apparent from the unusual isomer shift of the tetrahedral M-center site,⁴ which exhibits neither the shift of a typical ferrous nor a typical ferric tetrahedral site. Finally, in comparing the cofactor iron sites with those of **1** and **2**, it should be noted that both model complexes exhibit substantially larger anisotropies of the magnetic hyperfine interactions than any of the cofactor sites.^{4,5} Clearly, the

(27) In deriving the value for P , we have assumed that the orbital contribution, A_{L} , can be computed by obtaining g_{\perp} from eq 5; if, for instance, g_{\perp} had the value 2.16 instead of 2.20, we would obtain $P = 59$ MHz and $\kappa = 0.35$. The reduction of the contact interaction could then possibly arise from a small 4s population, and P of **1** would be the same as the P -value of Fe^{II} rubredoxin.

(28) (a) Gismelseed, A.; Bominaar, E. L.; Bill, E.; Trautwein, A. X.; Winkler, H.; Nasri, H.; Doppelt, P.; Mandon, D.; Fischer, J.; Weiss, R. *Inorg. Chem.* **1990**, *29*, 2741. (b) Gupta, G. P.; Lang, G.; Lee, Y. J.; Scheidt, W. R.; Shelly, K.; Reed, C. A. *Inorg. Chem.* **1987**, *26*, 3022. (c) Ikeue, T.; Yamaguchi, G. *Chem. Commun. (Cambridge)* **2000**, *20*, 1989. (d) Mansuy, D.; Morgenstern-Badarau, I.; Lange, M.; Gans, P. *Inorg. Chem.* **1982**, *21*, 1427. (e) Reed, C. A.; Mashiko, T.; Bentley, S. P.; Kastner, M. E.; Scheidt, W. R.; Spertalian, K.; Lang, G. *J. Am. Chem. Soc.* **1979**, *101*, 2948.

(29) Fitzsimmons, B. W.; Johnson, C. E. *Chem. Phys. Lett.* **1974**, *24*, 422.

(30) (a) Collins, T. J.; Fox, B. J.; Hu, Z. G.; Münck, E.; Kostka, K.; Rickard, C. E. F.; Wright, L. J. *J. Am. Chem. Soc.* **1992**, *114*, 8724. (b) Kosta, K. L.; Fox, B. G.; Hendrich, M. P.; Collins, T.; Clifton, E. F.; Wright, L. J.; Münck, E. *J. Am. Chem. Soc.* **1993**, *115*, 6746.

(31) MacDonnell and collaborators have reported $\Delta E_{\text{Q}} = 2.53$ mm/s and $\delta = 0.78$ mm/s (at 4.2 K) for the $[\text{Fe}_2(\text{SC}_6\text{H}_2\text{-2,4,6-tBu}_3)_4]$. This centrosymmetric complex has ostensibly three-coordinate iron sites, and thus the larger ΔE_{Q} and δ values would seem to be puzzling. However, Evans et al.³² have pointed out that, because of interactions between the iron and the carbons/ π clouds of the phenyl rings, the iron environment is best described as distorted tetrahedral four-coordinate.

(32) Evans, D. J.; Hughes, D. L.; Silver, J. *Inorg. Chem.* **1997**, *36*, 747.

(33) Yoo, S. J.; Meyer, J.; Münck, E. *J. Am. Chem. Soc.* **1999**, *121*, 10450.

(34) Yoo, S. J.; Hayley, A. C.; Burgess, B. K.; Hendrich, M. P.; Münck, E. *J. Am. Chem. Soc.* **1999**, *121*, 2534.

present study is only a beginning in our efforts to understand the electronic structure of the nitrogenase cofactor.

While this paper was reviewed, Lovell et al. reported calculations of the nitrogenase cofactor using broken-symmetry density functional theory.³⁵ The authors conclude that “Fe–Fe bonding is inherently moderately weak” within the M cluster suggesting that A-values and zero-field splittings obtained for suitable monomers can be transferred into the spin-coupling problem of the cofactor. Lovell et al. have calculated the A-values of the cofactor Fe sites using various coupling models. For these calculations, the authors used for the ferrous “trigonal” sites A-values around –22 MHz (L. Noodleman, personal communication), obtained by calculating A for the free ferrous ion and using covalency corrections obtained from DFT of the cofactor. Given our result for the A-value of **1**, A-values of –22 MHz seem quite

(35) Lovell, T.; Li, J.; Liu, T.; Case, D. A.; Noodleman, L. *J. Am. Chem. Soc.* **2001**, *123*, 12392.

large. However, the DFT calculations indicate, for six of the seven Fe sites, ligand field splittings substantially larger ($\geq 8000\text{ cm}^{-1}$) than the 3000 cm^{-1} estimated here for **1**. If the cofactor iron sites would indeed have substantially larger ligand field splittings than **1**, they would have smaller D-values and thus smaller orbital contributions to the A-tensor. However, in our experience, DFT calculations tend to overestimate the orbital splittings, and thus, it will be important to determine the ligand field splittings of **1** by optical spectroscopy and compare the results with the theoretical estimates. Such studies, using low-temperature MCD, are in preparation.

Acknowledgment. This work was supported by National Science Foundation Grant MCD-9416224 (E.M.) and the Petroleum Research Fund administered by the American Chemical Society (P.P.P).

IC0111278